Polymer Bulletin 62, 45–55 (2009)
DOI 10.1007/s00289-008-1011-x

Polymer Bulletin

Evaluation of a composite based on high-density polyethylene filled with surface-treated hydroxyapatite

Albano C.[1,2] (✉), Cataño L.[1], Figuera L.[2], Perera R.[3] (✉), Karam A.[1], González G.[4], Noris K.[5]

[1] Laboratorio de Polímeros, Centro de Química, Instituto Venezolano de Investigaciones Científicas, Caracas, Venezuela.
[2] Universidad Central de Venezuela, Facultad de Ingeniería, Escuela de Ingeniería Química, Caracas, Venezuela.
[3] Departamento de Mecánica, Universidad Simón Bolívar, Valle de Sartenejas, Caracas, Venezuela.
[4] Departamento de Ingeniería, Instituto Venezolano de Investigaciones Científicas, Caracas, Venezuela.
[5] Universidad Simón Bolívar, Valle de Sartenejas, Caracas, Venezuela.
E-mail: calbano@ivic.ve; rperera@usb.ve

Received: 13 June 2008 / Revised version: 6 October 2008 / Accepted: 6 October 2008
Published online: 20 October 2008 –

Summary

Composites properties are directly related to the degree of interaction between the plastic matrix and the inorganic filler. In the present work, the improvement of the composite's properties by means of the addition of surface-treated and untreated hydroxyapatite (STHA and HA, respectively) was studied. An ethylene-acrylic acid copolymer was melt blended with high-density polyethylene and HA (HDPE/HA/EA). A surface treatment was performed using an ethylene-acrylic acid (EA) copolymer for $STHA_1$ and acrylic acid (AA) for $STHA_2$. High-density polyethylene (HDPE) was also tested. $STHA_1$ and $STHA_2$ composites exhibited Young's modulus values (556 and 558 MPa, respectively) 22 % higher than that of HDPE/HA (455 MPa) and 8 % higher than that of HDPE/HA/EA (520 MPa). Additionally, STHA composites showed both yield stress and strain (σ_{STHA1}= 23 MPa; ε_{STHA1}= 9 %; σ_{STHA2}= 22 MPa; ε_{STHA2}= 10 %) having a remarkably different behavior from that of the HA composites, which showed no yielding at all. TEM micrographs showed better filler dispersion when surface treatment was applied to HA. Yet, the presence of EA copolymer exhibited a poorer thermal stability. The crystallinity degree as well as the crystallization and melting temperatures showed no significant variation. Regarding *in vitro* evaluation, composites with HA and EA copolymer proved to have better cell adhesion at early stages. The results of the STHA composites could be attributed to the electrostatic interactions taking place between the ethylene-acrylic acid copolymer and the polar groups of the HA.

Introduction

Polyolefins are materials with a widespread range of applications due to their properties, versatility and low cost. From the toy industry to complex engineering applications,

these materials have exhibited an outstanding performance. However, because of their mechanical properties, there are many areas in which the use of polyolefins is limited. For example, applications requiring properties such as toughness and resistance are hard for these materials to fulfill. Therefore, rigid particulated fillers are being incorporated into the polyolefin matrix in order to promote mechanical strength. For instance, hydroxyapatite (HA) reinforced polyethylene (PE) is revealing a potentially increasing performance as a biomaterial because of its resemblance to bone physical properties[1-3].
In general, every composite show a behavior directly related to the combination of the properties of both of the compounds, i.e. matrix-filler interaction. Thus, it is of significant importance to deal with the interfacial strength of the composite.
Recent work has used unsaturated monomers such as acrylic acid (AA) in order to be grafted onto PE promoting interfacial adhesion when HA is employed as filler[4-6]. Wang & Bonfield[4] reported an increase in ductility and tensile strength of AA-grafted high-density polyethylene (HDPE) composites filled with HA. Additionally, Huang[5] et al. promoted HA biomineralization in the PE when grafted with AA, improving the mechanical properties of the composite as well. Thus, increasing the interfacial strength by adding functionality to the PE is seen as an achievable goal.
However, looking for the ultimate goal, i.e. improving mechanical properties, the material biocompatibility can be utterly affected. Therefore, it is of significant importance to enhance mechanical properties making sure not to diminish the biocompatibility. For instance, Di Silvio[7] demonstrated that osteoblastic cell attachment and bone in-growth could be carried out controlling the composition as well as the surface topography of the HA in HDPE composites. Moreover, Zhang[8] et al. showed that HDPE composites filled with 60 wt % HA evidenced a regular growing cycle of osteoblast cells. Authors evaluated unfilled PE, HA and their composites, to then prove that the best *in vitro* response belong to the latter. They conclude that HDPE filled with 60 wt % HA, combined with its excellent mechanical properties, showed to be a potential candidate as a biomaterial.
Therefore, in the present work, morphological, biological and mechanical properties of 30 wt % HA filled HDPE were evaluated with and without the addition of an ethylene-acrylic acid (EA) copolymer which brings functionality into the PE matrix, improving the interfacial strength of the composites. In addition, this material is also compared to a HDPE composite filled with a surface-treated HA (STHA).

Materials and Methods

A commercial HDPE was supplied by Polinter (MFR = 5 dg/min, ρ = 0,94 g/cm^3); an EA random block copolymer with 20 wt % of AA content and AA were supplied by Sigma-Aldrich. Calcium hydroxide was purchased from Mallinckrodt and ammonium phosphate was supplied by Fischer Scientific. Decalin was supplied by Riedel-de Haën. Triethanol amine was provided by Aldrich. Reagents and materials for cell culture and tests were purchased from the following sources: Dulbeco's Modified Eagle's Medium (DMEM), trypsin and fetal bovine serum (FBS) GIBCO, penicillin, streptomycin and collagenase, SIGMA. CyQuant kit was purchased from Invitrogen.

Synthesis of HA

HA granules were prepared trough a precipitation reaction between calcium hydroxide ($Ca(OH)_2$) and ammonium phosphate ($(NH_4)_2HPO_4$) solutions, according to a method

described in the literature[9]. The resulting solution was centrifuged and washed with deionized water until neutral pH to finally being vacuum dried for 48 hours at 65 °C. HA was then milled and sieved with a 150-mesh screen. The resulting powder was subjected to a particle size- distribution analysis which evidenced a mean particle size of 6.9 µm. Size distribution is shown on figure 1.

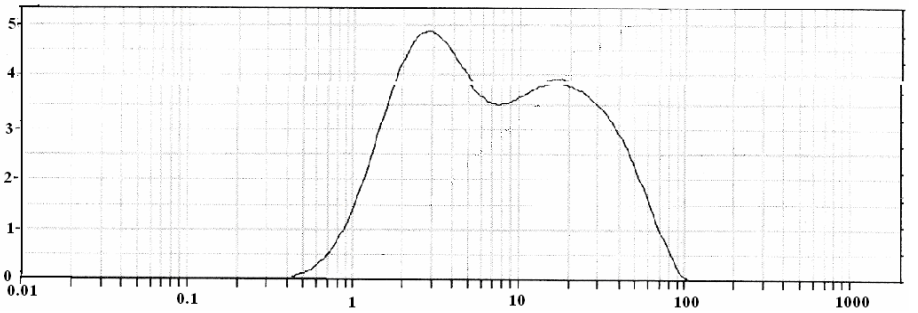

Figure 1. Particle size distribution of HA powder used in compounding.

Composite Preparation

Composites were prepared in a Haake Rheomix internal mixer. HDPE was added to the mixing chamber at 160 °C at a rotors rate of 50 rpm. Subsequently, EA copolymer was added in 2 phr according to the HDPE matrix. Finally, HA was added at the corresponding amount in order to have 30 wt %. The screw ratio was increased to 90 rpm for 8 min. Material references can be seen in table 1.

Table 1. Material reference

Material	Code
High-density polyethylene with 30 wt % of hydroxyapatite	HDPE/HA
High-density polyethylene with 30 wt % of hydroxyapatite and 2 phr of ethylene-acrylic acid copolymer with 20 wt % of acrylic acid.	HDPE/HA/EA
High-density polyethylene with 30 wt % of EA-copolymer-surface-treated hydroxyapatite	$STHA_1$
High-density polyethylene with 30 wt % of AA-surface-treated hydroxyapatite	$STHA_2$

HA Surface Treatment

Surface Treatment with EA Copolymer. HA surface treatment was carried out in solution, where 1 g of EA copolymer was dissolved during a 20 minute-period in 200 ml of decalin heated at 130 °C under continuous stirring. After that, the temperature was lowered to 80 °C. Triethanolammine (TEA) was then added to the solution (1 ml) and left apart for about 10 more minutes. HA powder (about 15 g) was incorporated to that final solution and the stirring kept for another 20 minutes. The solution was washed with ethanol and then vacuum filtered. The slurry was then vacuum-dried at

80 °C for 48 h in order to remove the solvent. The resulting powder was prepared for compounding.

AA Surface Treatment. Initial conditions were similar to the above mentioned procedure. First, 0.5 mL of AA was added to the decalin solution at 80 °C for 10 min. After that, 1 ml of TEA was incorporated into the solution. The following steps were the same described before.

Biocompatibility Test

Osteoblast preparation. Osteoblasts were isolated from 12 calvaria of 2-3 day-old neonatal rats as in a previous article described by Noris et al[10]. Calvaria was dissected under aseptic conditions and freed from soft tissue except for periosteal coverings, followed by several phosphate-buffered (PBS) washes. Enzymatic digestion of tissue was obtained using 1 mg/ml collagenase, 0.125 % trypsin and 0.5 mM EDTA. Cells corresponding to the 3rd digestive extraction were seeded at a $6x10^5$ cells/dish density in 100-mm Petri dish and cultured with DMEM medium (completed with 10 % Fetal Bovine Serum, 100 U/ml penicillin and 100 µg/ml streptomycin). Cells were maintained at 37 °C in a fully humidified atmosphere at 5 % CO_2 in air. The media was first changed 7 days after culturing and after this initial change, every 3-4 days until cells reached confluence.

Adhesion and proliferation tests. The different materials to be tested were treated with 70 % ethanol to remove the superficial grease. Then they were washed extensively with deionized water and finally sterilized with a 25 kGy gamma radiation dose. Spot samples of 6 mm diameter were tested using a 96 well-plate (for tissue culture, NUNC). The cell number on the materials and controls were determined using a commercial kit (CyQuant) following the instructions of the manufacturer. A $3x10^3$ cells/ml suspension was seeded with the different materials and control (which corresponds to an empty well). After 16 h of incubation in optimal culture conditions (37 °C in a fully humidified atmosphere at 5 % CO_2 in air), adhered cells were quantified using the CyQuant kit.

To evaluate viability for a longer period of time and proliferation, cells were cultivated in the same conditions described previously, for a period of 8 days, and the number of cells present in the samples was calculated employing the CyQuant kit.

Characterization

Tensile Tests. Tensile tests were performed in an Instron 4204 universal testing machine. Type V sample specimens (ASTM D-638) were cut from a 1 mm-thin plate which was compress-molded. Tests were carried out using a crosshead speed of 50 mm/min.

Differential Scanning Calorimetry (DSC). Differential scanning calorimetry analysis was carried out in a Mettler-Toledo DSC 822^e, under nitrogen gas, at a flow rate of 50 mL/min. Samples (9-10 mg) were heated up to 170 °C and subsequently kept for about 3 min in order to erase the previous thermal history. This initial heating was performed at a rate of 20 °C/min. Then, the samples were subjected to a cooling step down to room temperature and subsequently heated up to 170 °C, both at the same rate of 10 °C/min. Parameters were determined from the cooling and second heating. Crystallinity degree was calculated using the following formula:

$$Xc(\%) = \frac{\Delta Hm_{\exp}}{\Delta Hm_{theo}} \times 100 \quad (1)$$

Where Xc is the crystallinity degree, ΔHm_{exp} is the experimental melting enthalpy and ΔHm_{theo} corresponds to a 100 % crystalline PE, 293 J/g [11]. As HA is considered to be inert, the area of the peak was normalized to the actual content of PE.

Thermogravimetric Analysis (TGA). Thermal decomposition analyses were performed in order to elucidate the thermal stability of the samples evaluated. The E_2-function method, proposed by Chen[12] et al., was employed to calculate the activation energy (Ea). Samples (5-6 mg) were heated from room temperature up to 700 °C at a heating rate of 10 °C/min in a Mettler-Toledo TGA/STDA analyzer.

*Transmission Electron Microscopy (TEM).*Transmission electron microscopy (TEM) analyses were performed using a Phillips CM10 microscope. Samples were prepared by ultramicrotomy without any further conditioning.

Results and Discussion

Figure 2 shows the Young's modulus of the unfilled HDPE and the composites. As seen in this figure, the modulus increases with the addition of HA to the HDPE matrix. Furthermore, there is a moderate increase in the modulus when the EA copolymer is being added to the HDPE/HA composite, because it somehow affects the filler dispersion within the HDPE matrix. Moreover, when the HA is surface-treated with the EA copolymer and AA, a slight increase is being showed by the system.
On figure 2, it is worth to mention that the Young modulus increases with the addition of HA to the HDPE polymers. This states that the HA particles act as a reinforcement filler by transferring the sustaining load from the matrix to the rigid particles[13-15]. On STHA composites, it is supposed that the EA copolymer is activated by TEA used in the procedure, in order to link this molecule to Ca atoms in HA particles. This type of chemical bond is stronger than the one expected to be in melt-blended EA copolymer

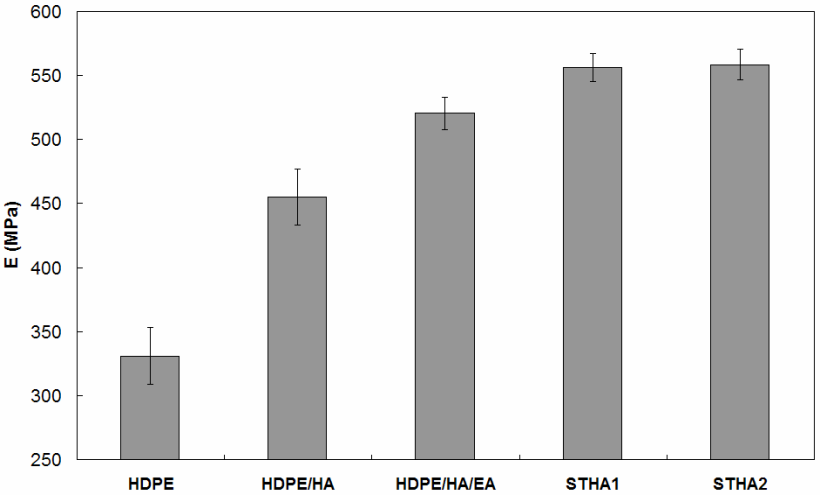

Figure 2. Young's modulus of HDPE and its composites.

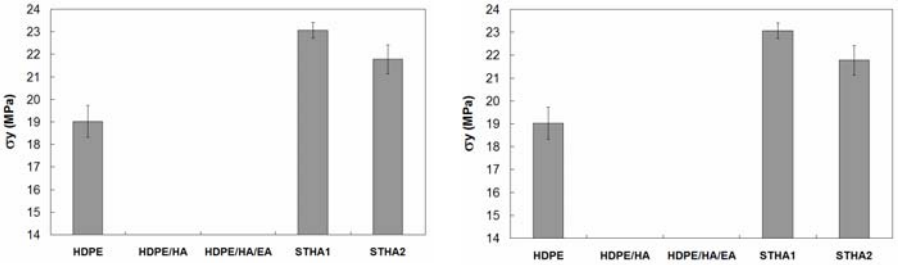

Figure 3. (a) Yield strength and (b) strain of HDPE and its composites.

and the HDPE/HA composite. Furthermore, it is noteworthy that the surface-treatment displays a higher efficiency due to the fact that this method is taking place in a decalin solution which allows the EA copolymer to make direct contact with the HA particles.
Regarding the tensile properties in yield shown in figure 3, both $STHA_1$ and $STHA_2$ showed yielding, exhibiting an opposite behavior from those composites with untreated HA at an equal level of filler loading. Yield strength values of STHA composites are slightly higher than those showed by the unfilled HDPE.
Concerning yielding properties, their behavior is attributed to the surface treatment applied to the HA particles. There could be a phenomenon occurring which explains this fact: matrix-filler stronger interactions could be taking place on the interface between the polymer and the HA particles which can be promoted by either the EA copolymer or the AA placed in the surface of the HA particles. It is relevant to consider that HA(Ca^{+2})-($^{2-}O_2C$)EA(or AA) bridges, as well as hydrogen bonds, are likely to be formed over the mechanical interlocking between the matrix and HA particles[16].
Figure 4 shows the tensile strength and strain values for the unfilled HDPE and its composites. As seen in this figure, tensile strength slightly increases in the STHA composites compared to those with untreated HA and the unfilled HDPE.

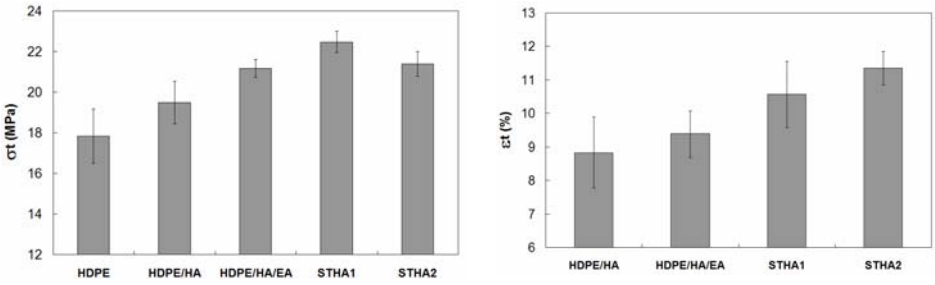

Figure 4. (a) Tensile strength and (b) strain of HDPE and its composites.

Stress-strain curves for the composites are depicted in figure 5. These curves were recorded at a crosshead speed of 1 mm/min. The STHA composite registered in the figure is the $STHA_1$. As it is well known, tensile properties values change with the deformation rate. However, Young's modulus values remain the same. As seen in the figure, the trend remains the same, i.e., an increased Young's modulus, yield and tensile strength of the STHA composites over the untreated-HA ones.

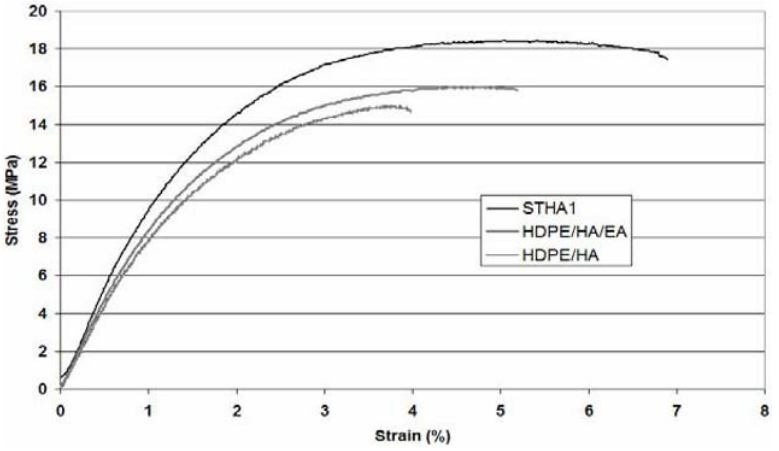

Figure 5. Stress-strain curves for different HDPE-HA composites at 1 mm x min-1

The increase underwent by the tensile strength and strain could be attributed to the EA and AA molecules placed in the surface of the HA particles; this supposes a decrease in the extent of the particle agglomeration, which contributes to reduce the effect of the stress concentration points around particles, which end up in premature failure by void formation upon stress loading, allowing them to transfer the tensile load in an efficient manner compared to those composites with untreated HA. On figure 5, $STHA_1$ curve denotes a higher area under the curve which represents a tougher mechanism of load transfer, probably due to the before-mentioned reasons.
Transmission electron microscopy (TEM) was performed in order to study the HA particle dispersion in the composites. As figure 6a depicts, due to the ductility displayed by the unfilled HDPE, there are folds produced by the material stretching

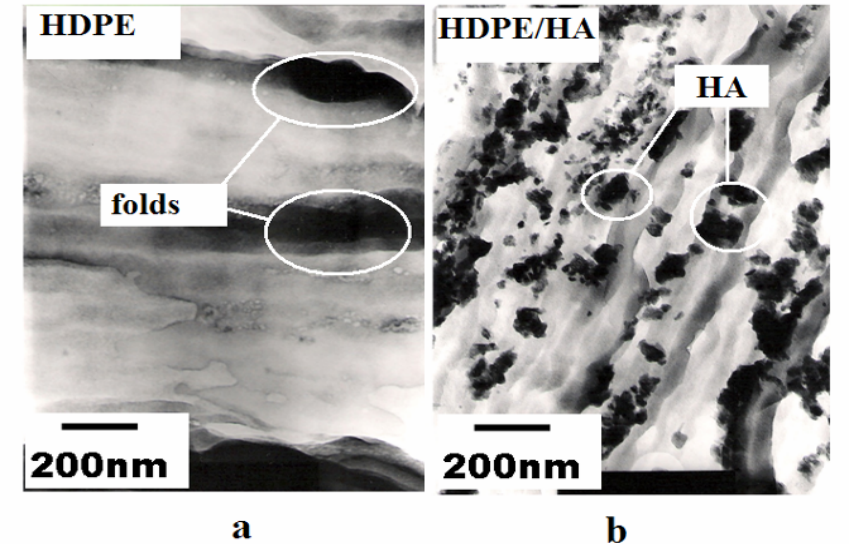

Figure 6. TEM micrographs of (a) HDPE and (b) HDPE-HA composites.

which are associated to the sample-cutting procedure. However, in figure 6b, HA particles can actually be observed through the entire PE matrix.
As seen on TEM micrographs, it is possible to distinguish the particle agglomeration phenomenon which is attributed to the compounding process as well as the lack of interaction between the PE matrix and the HA particles. Nevertheless, the addition of the EA copolymer in the compounding process results in better HA-particle dispersion. Figure 7 shows the HDPE/HA/EA micrograph, which evidences (at the same magnification of the previous figures) the presence of an enhanced dispersion, in addition to smaller aggregations of HA particles. STHA micrographs are shown in figure 8. Surface treatment performed on HA powder has resulted on a much more enhanced dispersion compared to that in HDPE/HA and HDPE/HA/EA composites as seen in the figure. TEM results evidenced a much more enhanced dispersion of the STHA composites, which is due to the efficient EA copolymer interfacial interaction taking place between the PE matrix and the HA particles. Moreover, this improvement is also in agreement with the tensile test results showed before.

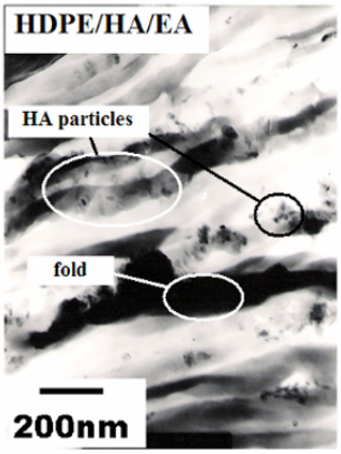

Figure 7. TEM micrograph of HDPE-HA-EA composite.

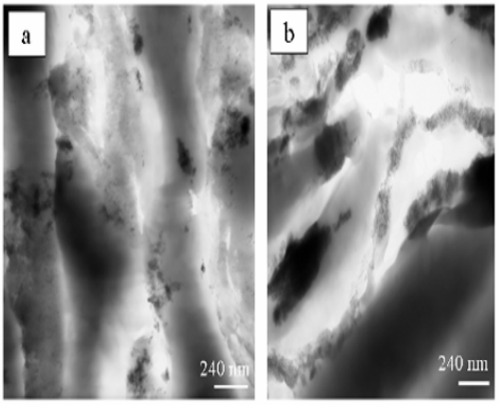

Figure 8. TEM micrographs of (a) STHA1 and (b) STHA2 composites

Differential scanning calorimetry analyses were carried out to study the influence of the EA copolymer and HA particles in the crystalline structure of the HDPE matrix. Figure 9 shows the melting peaks of the composites, evidencing that there is no significant variation in their position. Regarding crystallization and melting temperatures, there is no considerable change in their values; the same occurs with the crystallinity degrees (Table 2). Thermal decomposition of the unfilled HDPE and composites were evaluated employing thermogravimetric analysis (TGA). As table 2 shows, the Ea values increase with the addition of HA to the HDPE matrix which is reasonable due to the difference in the thermal stability between the HA ceramic and the HDPE polymeric matrix. However, the addition of either the EA copolymer or AA to the composite decreases the thermal stability. TGA results showed that there is a less thermally stable EA copolymer, which is prone to thermal degradation at relatively lower temperature due to the presence of a high content of carboxylic groups.

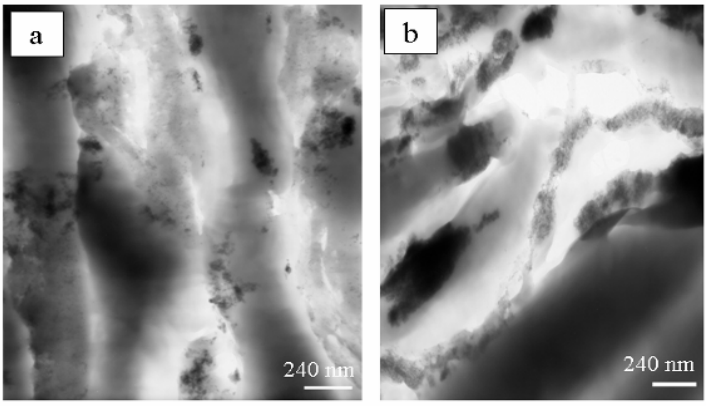

Figure 8. TEM micrographs of (a) STHA1 and (b) STHA2 composites

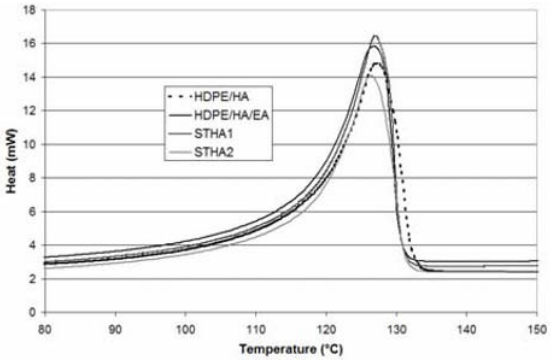

Figure 9. DSC melting peaks of composites

Table 2. Parameters calculated from HDPE and its composite's DSC and TGA thermograms.

Material	ΔH_m (J/g)	T_m (°C)	T_c (°C)	X_c (%)	E (kJ/mol)
HDPE	172	126	112	59	372
HDPE/HA	174	127	112	59	437
HDPE/HA/EA	164	127	111	56	338
$STHA_1$	174	127	110	60	314
$STHA_2$	157	126	110	54	335

Biocompatibility results are shown on figure 10. Due to the presence of HA in the composites, cell adhesion on those samples increased related to the HDPE values. However, surface-treated samples evidenced the opposite behavior by diminishing the biocompatibility.

Concerning biocompatibility test, after the first 16 hours, there was a visible cellular recognition on the surface of the HDPE sample as well as on the composites without surface treatment. Despite of the lack of polar groups in PE, which are very attractive to cell proliferation at material surface, there is some sort of adhesion. In addition, the HDPE/HA composite exhibits a slightly higher value of cell adhesion which is attributed to the presence of polar groups in the HA contained in the sample.

However, the presence of the bioactive filler seems not to increase the cell adhesion, possibly because the particles are located deep inside the sample.
On the other hand, figure 10 shows that the cell adhesion is being favored by the presence of the EA copolymer in HDPE/HA/EA composites. AA molecules in the EA copolymer promote a higher cell proliferation in the composite, which is proven by the difference in the values of the composites with and without EA copolymer.

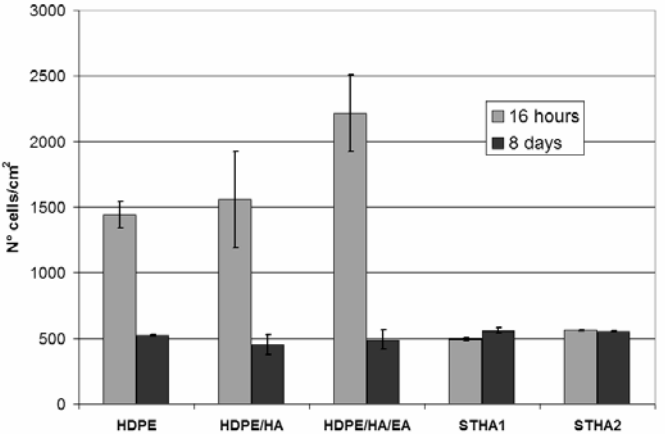

Figure 10. Cell adhesion test of HDPE and its composites at 16 hours and 8 days.

Therefore, the HDPE/HA/EA composite shows a better cell adhesion because of the acrylic acid content in the EA copolymer used. The effect shown by these groups is due to the cell recognition towards the hydrophilicity of the molecules at the material's surface. Mizuno[17] et al. showed that this recognition is related to the presence of polar groups in biological fluids and proteins, such as collagen, which supports preosteoblast attachment. Moreover, Mizuno[18] et al. found that this behavior towards polar groups tends to be highly significant to cells in early stages of differentiation, such as preosteoblastic cells.
Regarding STHA composites, cell adhesion on early stages is strongly reduced compared to the rest of the materials. STHA seems to have a strong influence on cell adhesion, which is attributed to the lower number of free polar groups, linked to each other in the surface treatment. Hydroxyl groups, along with calcium atoms of HA, could be interacting with the acrylate groups of the EA copolymer leaving less chance to the cells to survive. In the lack of these groups, cells might not have any chemical bond to link to, which is a possible explanation to these behaviors.
Regarding long-term cell adhesion (Figure 10), results show that there is a tendency to cell death in the HDPE and the composites. However, STHA samples showed no variation on their cell number. This behavior could be due to a factor inherent to the samples, which is influencing the cell long-term adhesion.

Conclusions

The incorporation of EA copolymer as well as STHA showed to have a remarkable effect in the mechanical properties of composites. TEM micrographs showed better

filler dispersion when surface treatment was applied to HA. Furthermore, STHA samples displayed an increase in the Young's modulus and also unfolded yielding. Yet, the presence of the EA copolymer exhibited a poorer thermal stability. The crystallinity degree, as well as the crystallization and melting temperatures, showed no significant variation. Regarding *in vitro* evaluation, composites with HA and EA copolymer showed to have better cell-adhesion response compared to those without copolymer. The results of the STHA composites could be attributed to the electrostatic interactions taking place between the acrylate groups, in EA copolymers and AA, and the polar groups of the HA.

References

1. Wang M, Porter D, Bonfield W (1994) British Ceramic Transactions 93: 91
2. Tanner KE, Downes RN, Bonfield W 1994 British Ceramic Transactions 93:104
3. Wang M, Berry C, Braden M, Bonfield W (1998) Journal of Materials Science: Materials in Medicine 9:621-624
4. Deb S, Wang M, Tanner KE, Bonfield W. *Journal of Material Science: Materials in Medicine.* 1996; 7: 191
5. Wang M, Bonfield W (2001) Biomaterials 22:1311
6. Huang S, Zhou K, Zhu W, Huang B, Li Z (2006) Journal of Applied Polymer Science 101:1842
7. Di Silvio L, Dalby MJ, Bonfield W (2002) Biomaterials 23:101
8. Zhang Y, Tanner KE, Gurav N, Di Silvio L (2007) Journal of Biomedical Material Research 81A:409
9. Spadavecchia U, González G, Villalba R (2001) in Proc. VI CIASEM, Veracruz, Mexico
10. Noris Suarez K, Barrios de Arenas I, Vasquez M, Baron Y, Atias I, Bermudez J, Morillo C, Olivares Y, Lira-Olivares J (2003) Latin American Journal of Mettalurgy and Materials 23:82
11. Lim KLK, Mohd Ishak ZA, Ishiaku US, Fuad AMY, Yusof AH, Czigany T, Pukanzsky B, Ogunniyi DS (2006) Journal of Applied Polymer Science 100:3931
12. Chen HJ, Lai KM, Lin YC (2004) Journal of Chemical Engineering Japan 37:1172
13. Wang M, Deb S, Bonfield W (2000) Materials Letters 44: 119
14. Shahbazi R, Javadpour J, Khavandi AR (2006) Advances in Applied Ceramics 105:253
15. Pandey A, Jan E, Aswath PB (2006) Journal of Material Science 41:3369
16. Pramanik N, Mohapatra S, Pramanik P, Bhargava P (2007) Journal of American Ceramic Society 90:369
17. Mizuno M, Kitafima T, Tomita M, Kuboki Y (1996) Biochimica et Biophysica Acta (BBA) - Molecular Cell Research 1310:97
18. Mizuno M, Fujisawa R, Kuboki Y (2000) FEBS Letters 479:123